Solar Phys (2010) 262: 213–231
DOI 10.1007/s11207-010-9513-8

Background Subtraction for the SECCHI/COR1 Telescope Aboard STEREO

W.T. Thompson · K. Wei · J.T. Burkepile · J.M. Davila · O.C. St. Cyr

Received: 24 August 2009 / Accepted: 11 January 2010 / Published online: 4 February 2010

Abstract COR1 is an internally occulted Lyot coronagraph, part of the Sun Earth Connection Coronal and Heliospheric Investigation (SECCHI) instrument suite aboard the twin *Solar Terrestrial Relations Observatory* (STEREO) spacecraft. Because the front objective lens is subjected to a full solar flux, the images are dominated by instrumental scattered light which has to be removed to uncover the underlying K corona data. We describe a procedure for removing the instrumental background from COR1 images. F coronal emission is subtracted at the same time. The resulting images are compared with simultaneous data from the Mauna Loa Solar Observatory Mk4 coronagraph. We find that the background subtraction technique is successful in coronal streamers, while the baseline emission in coronal holes (*i.e.* between plumes) is suppressed. This is an expected behavior of the background subtraction technique. The COR1 radiometric calibration is found to be either 10 – 15% lower, or 5 – 10% higher than that of the Mk4, depending on what value is used for the Mk4 plate scale, while an earlier study found the COR1 radiometric response to be ∼20% higher than that of the Large Angle Spectroscopic Coronagraph (LASCO) C2 telescope. Thus, the COR1 calibration is solidly within the range of other operating coronagraphs. The background levels in both COR1 telescopes have been quite steady in time, with the exception of a single contamination event on 30 January 2009. Barring too many additional events of this kind, there is every reason to believe that both COR1 telescopes will maintain usable levels of scattered light for the remainder of the STEREO mission.

W.T. Thompson (✉)
Adnet Systems Inc., NASA Goddard Space Flight Center, Code 671, Greenbelt, MD 20771, USA
e-mail: William.T.Thompson@nasa.gov

K. Wei
Adnet Systems Inc., University of Maryland, 7515 Mission Drive, Lanham, MD 20706, USA

J.T. Burkepile
High Altitude Observatory, National Center for Atmospheric Research, P.O. Box 3000, Boulder, CO 80307, USA

J.M. Davila · O.C. St. Cyr
NASA Goddard Space Flight Center, Code 671, Greenbelt, MD 20771, USA

Keywords Instrumental effects · Corona · STEREO · COR1

1. Introduction

All solar coronagraphs exhibit some level of instrumental scattered light which must be removed from the data to derive the true coronal intensity. This is particularly true for internally occulted coronagraphs, such as the COR1 telescopes which are part of the Sun Earth Connection Coronal and Heliospheric Investigation (SECCHI) (Howard *et al.*, 2008) aboard the *Solar Terrestrial Relations Observatory* (STEREO). An earlier work described the radiometric and pointing calibration of COR1 (Thompson and Reginald, 2008), hereafter referred to as Paper I, but did not discuss the process of background subtraction. Instead, pre-event images were used to isolate coronal mass ejections (CMEs) from both the instrumental background, and from the surrounding coronal streamers. This technique works well for transient events such as CMEs, which is what COR1 was designed to study. However, there is also considerable interest within the solar physics community in using COR1 data to study non-transient coronal structures such as streamers and polar plumes. For such studies, a reliable background subtraction method is needed. This paper outlines the methods used to derive the time-dependent COR1 instrumental background, and compares the resulting coronal images to other measurements of the K corona.

The details of the COR1 design are described elsewhere (Howard *et al.*, 2008; Thompson *et al.*, 2003). In brief, COR1 is a classic Lyot internally occulting refractive coronagraph (Lyot, 1939), adapted for the first time to be used in space. The field of view ranges from 1.4 to 4 solar radii. A bandpass filter restricts the wavelength range to a region 22.5 nm wide, centered on the Hα line at 656 nm. The detector is a 2048 × 2048 CCD with 3.75 arcseconds per pixel. Because of telemetry considerations, most data are binned to either 1024 × 1024 or 512 × 512, with corresponding plate scales of either 7.5 or 15 arcseconds per pixel respectively. Spacecraft pointing is maintained to an arcsecond or better through a guide telescope on the same optical bench as COR1 and the other SECCHI Sun-pointed telescopes.

Because the front objective lens of COR1 is subjected to a full solar flux, the images are dominated by instrumental scattered light which has to be removed to uncover the underlying K corona data. Figure 1 shows the total brightness (B) and polarized brightness (pB) derived for a typical COR1 observation sequence when no background subtraction is applied. Also, as is the case with all the figures in this paper, instrumental vignetting has not been applied so as to represent the raw signal reaching the detector. The instrumental scattered light is so dominant that no coronal features are evident in B. The situation is different for pB; the stray light is only weakly polarized, so that the strongly polarized K corona can be made out, even without subtracting off the background. However, there is still a substantial polarized stray component which needs to be removed for the scientific use of the data.

The pre-launch requirement for COR1 was that the stray light be kept below $10^{-6} B/B_{\odot}$. Figure 2 demonstrates that this requirement was met and even exceeded for both COR1-A on STEREO-A, and COR1-B on STEREO-B. In addition to this diffuse scattering component are small bright ring-shaped features at various locations on the image. The brightest of these on COR1-B reaches $1.4 \times 10^{-6} B/B_{\odot}$, but only over a small area. These artifacts have been determined to be caused by features on or near the front surface of the field lens, probably created during the processing of the lens to attach the occulter stem. Since the field lens is before the Lyot stop, it is primarily illuminated by diffracted light from the edge of the

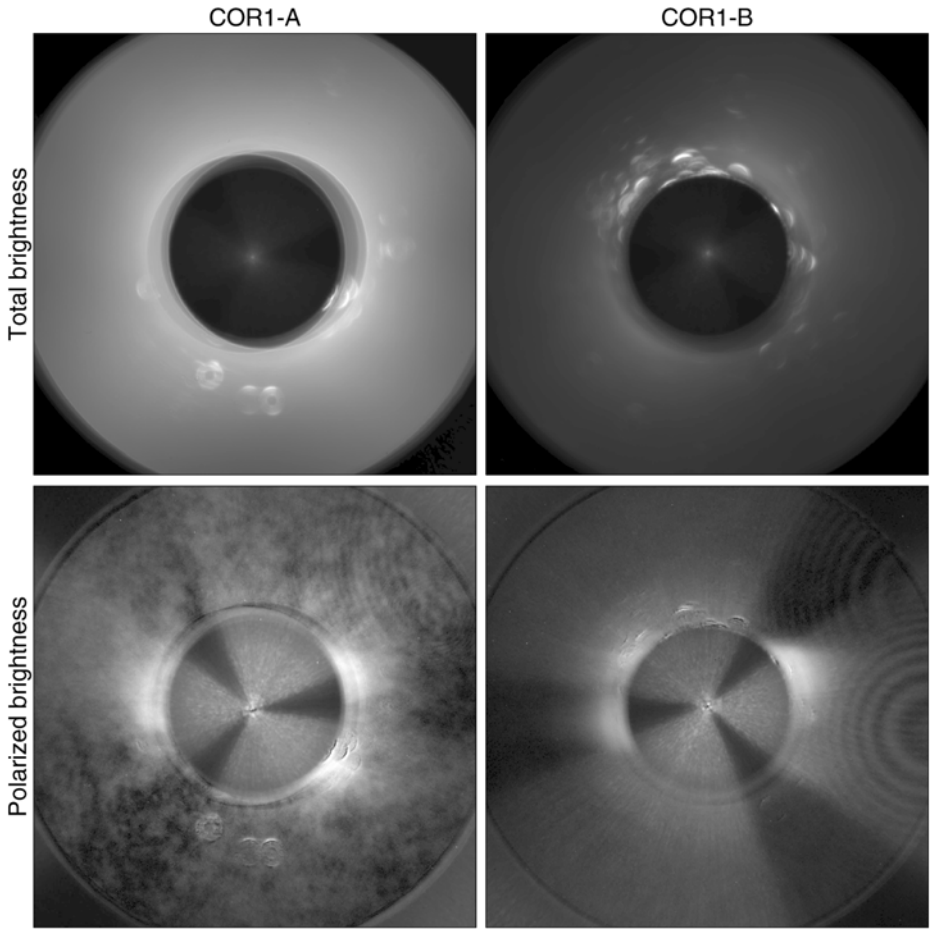

Figure 1 Total and polarized components of the raw COR1 signal for 3 June 2008. Some coronal features can also be discerned in the polarization images. The B and pB images are not on the same scale – the pB images are actually much fainter than the B images.

front aperture. The primary source of error in Figure 2 is the COR1 radiometric uncertainty of 10%. However, the relative radiometric uncertainty between COR1-A and COR1-B is only 1%, which is too small to show on the figure.

The polarized stray light pattern is dominated by three fan-shaped components reaching outward from the center of the occulter, and which are unobstructed by the occulter. These features most likely arise from the three attachment points at the edge of the field lens.

In addition to the instrumental stray light, and the K coronal light that the instrument is designed to detect, the COR1 signals also include a component from the Sun's F corona (dust corona). For the purposes of COR1 data analysis, the F coronal signal is treated as part of the overall scattered light pattern, and is subtracted off as part of the background to derive the K coronal signal. No attempt is made to extract the F corona as a separate signal, and indeed it may not be possible to do so.

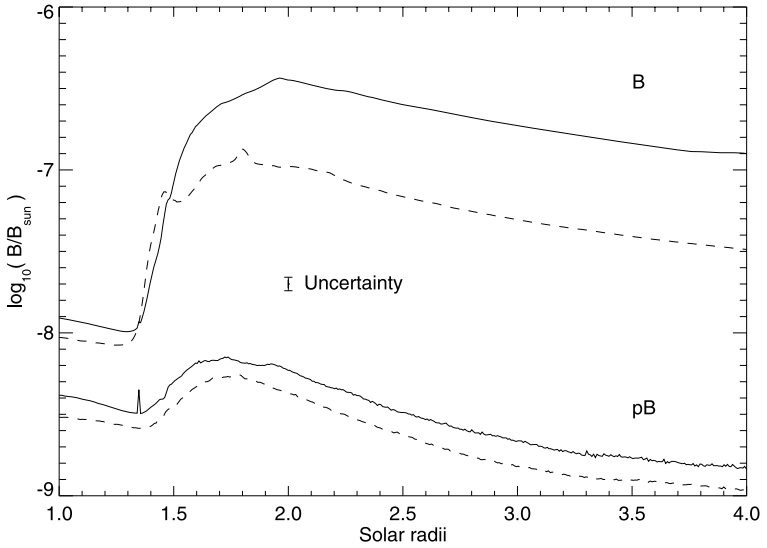

Figure 2 Average radial scattered light profile for the images in Figure 1 for COR1-A (solid) and COR1-B (dashed). The top two curves are for total brightness, and the lower two are for polarized brightness. The vignetting near the edge of the occulter has not been removed from these data. Error bar represents 10% radiometric uncertainty.

2. Daily and Monthly Backgrounds

The primary method used to isolate the K corona from the scattered light is to form background images derived from an examination of multiple images spanning a period of time. This is a modification of a technique used for the Large Angle Spectroscopic Coronagraph (LASCO), in which the backgrounds are generated from a combination of daily median images and monthly minimum images (Morrill *et al.*, 2006). The following sections describe how this technique was adapted for use by COR1.

2.1. Daily Background Images

The first step in the LASCO method is to generate daily median images formed by stacking all the images together into a data cube, and then taking the median value along the time dimension at each pixel position. The purpose of this procedure is to derive a representative image for each day, with most of the noise fluctuations removed, and without transient features such as CMEs. An alternative procedure would be to take the minimum along the time dimension instead of the median, so as to reject more of the K corona which is presumably evolving during the day. However, that would not be a truly representative image because it would be biased toward the low end of noise fluctuations, and thus would underestimate the amount of background to subtract.

A hybrid approach was adopted for COR1 which achieves a compromise between these two approaches. The observations in a given day are split up into M blocks of N images each. The segmentation is done so that M and N are approximately equal. For example, if the COR1 sequences are run with a 10 minute cadence, then the resulting set of 144 images would be split up into 12 blocks of 12 images each, with each block encompassing 2 hours of data. Within each block, a representative median image is generated as is done for LASCO.

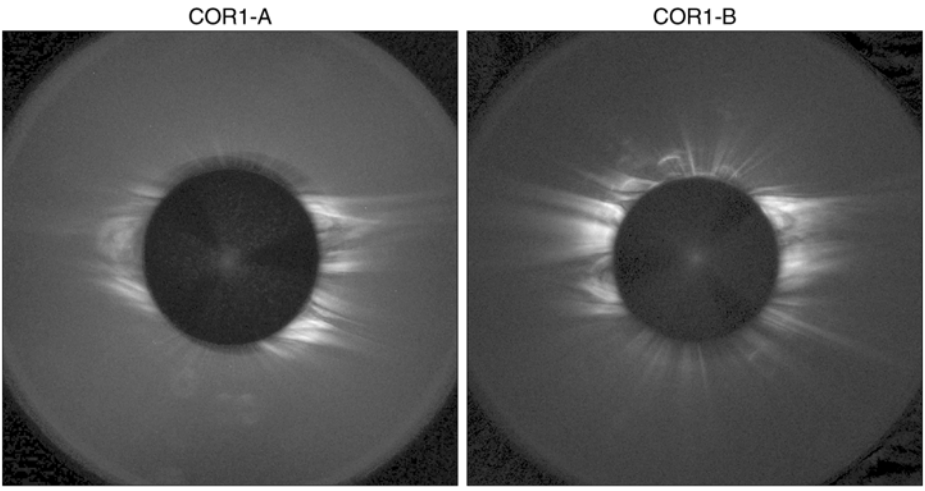

Figure 3 Difference images formed by subtracting a daily background image, generated using the technique described in Section 2.1, from a traditional daily median image, for 3 June 2008.

These M median images are then themselves combined into a data cube, and the minimum value is taken along the time dimension. The result is a daily "median" background image which approximates the correct statistical average, but with the evolving component of the K corona removed. Figure 3 shows the additional K coronal signal which is removed from the daily background images compared to the traditional LASCO daily median approach.

Background images are generated without any calibration factors applied to them, so that the background image files do not need to be regenerated if the calibration factors change. Thus, the backgrounds are not corrected for vignetting or flat fielding, and the values are not converted into mean solar brightness units. In the SECCHI software, which is distributed as part of the SolarSoft suite (Freeland and Handy, 1998), this is equivalent to calling `SECCHI_PREP` with the keywords `/CALIMG_OFF` and `/CALFAC_OFF`. The flat field and brightness calibration factors are applied to COR1 data *after* the background image is subtracted. So that the background polarization is treated correctly, separate backgrounds are generated for each of the polarizer settings, at 0°, 120°, and 240°.

The resulting daily background images still contain a significant contribution from the K corona. These can be applied to the data, but the primary reason for generating these daily backgrounds is to serve as input for generating the monthly minimum background images described in the next section. The hybrid procedure described here improved the monthly minimum background images compared to the traditional daily median approach. Subtracting the daily backgrounds can be useful though, if one wants to suppress most of the background corona to emphasize the transient features. However, while useful for highlighting morphology and structure, interpretation of the intensity results should be treated with caution. For example, subtracting a daily background would not be appropriate for tomographic reconstruction.

2.2. Monthly Minimum Images

The second step in the LASCO method is to take the daily median images, and process them into monthly minimum images. For a given date, the daily median images covering two

weeks on either side of the date are collected together into a data cube, and the minimum value for each pixel is derived. The resulting data cube covers a period of 29 days, *i.e.* about one month, hence the "monthly" appellation. These monthly minimum files are generated every 10 days for COR1, so each month will have around three sets of background files associated with it. Since 29 days is long enough to encompass a complete solar rotation, solar features will rotate in and out of the field of view of any given pixel in the image. By taking the minimum value over the time dimension, much of the K corona will be removed from the derived background image. However, the background will still contain any part of the K corona signal which persists over the 29 day period.

Some modifications were needed to apply this procedure to COR1, because the COR1 background has a slow but significant drift with time. Part of this change was determined to be a secular effect caused by the changing solar distance over the course of a spacecraft orbit, but the instrument profile also slowly evolves with time. This is discussed in more detail in Section 7. When processing a block of 29 days of data to form a monthly minimum, each of those daily images has to first be rescaled to a common brightness level. This is done by collecting the median value over all the pixels in each image, and then scaling that to the average over the 29 median values.

After the images have been rescaled, a check is made for images which appear anomalous. This is done by forming the difference between each image and the average of the neighboring images. The image is then split up into 100 intensity regimes between the minimum and maximum intensities of the original image. Within each regime, the root-mean-square difference is calculated, and any pixels with differences larger than three times that amount are marked as unusual. If a large number of pixels in an image is thus marked, *i.e.* three times more than the median number of marked pixels for all the images being considered, then the entire image is rejected. The remaining images are stacked together, and the minimum value at each pixel location is calculated to form a monthly minimum background image. Figure 4 shows the difference between the monthly and daily backgrounds, demonstrating that a substantial portion of the K corona has been rejected, in addition to that which

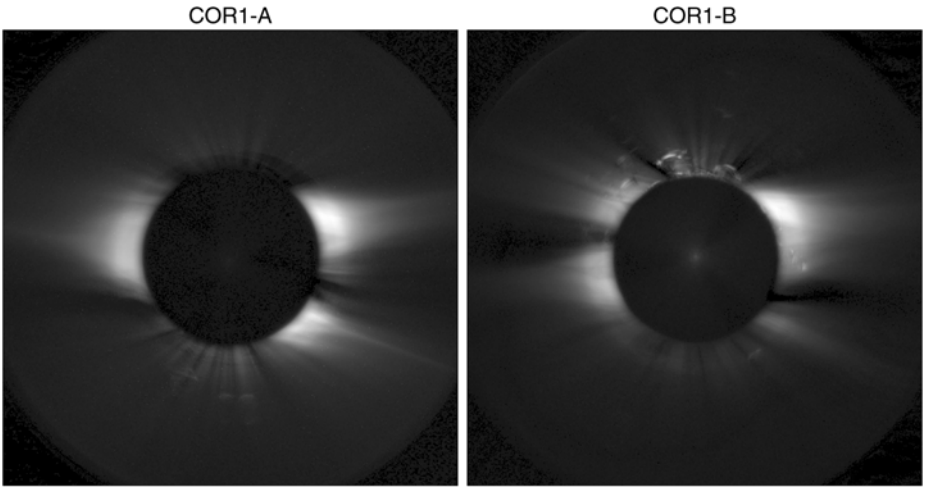

Figure 4 Difference images formed by subtracting a monthly minimum background image from a daily "median" background image, for 3 June 2008.

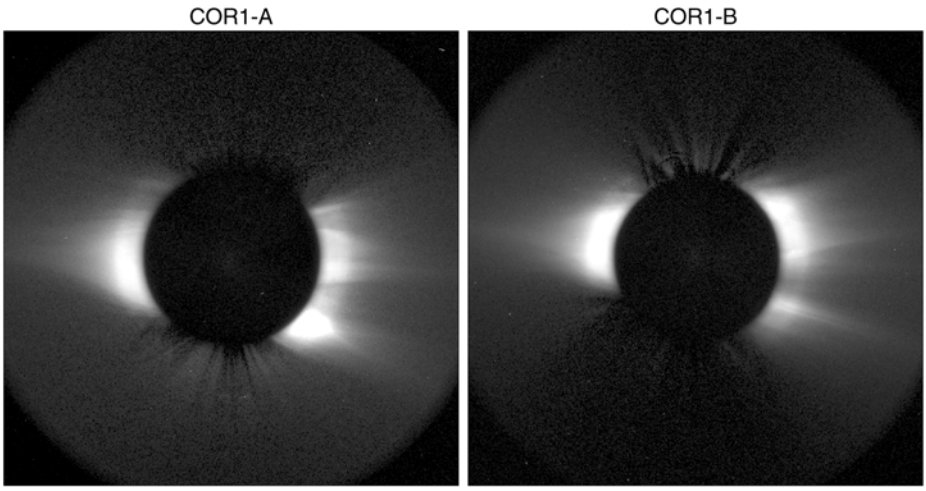

Figure 5 Calibration roll data with the minimum image subtracted as a background. COR1-A data are from 26 June 2008, and COR1-B data are from 25 June 2008.

has already been rejected in Figure 3. It is these monthly minimum backgrounds which are applied by default to COR1 data in the routine `SECCHI_PREP`.

3. Calibration Rolls

A completely different approach to deriving an instrumental background is to roll the spacecraft about the spacecraft-Sun axis. This is a standard maneuver which takes COR1 polarization sequence images at 60° intervals between 0° and 360°, plus stops at 90° and 270°. A roll minimum background is generated by stacking together the nine observations taken during the calibration roll maneuver and taking the minimum value at each pixel position. The resulting background image is free from any artifacts caused by persistent streamers. Instead, it depends on the existence of well-developed polar holes, which end up with base values (*i.e.* between plumes) close to zero brightness in this scheme. The use of this background image is demonstrated in Figure 5.

4. Combining Monthly Minimum and Calibration Roll Backgrounds

Since the COR1 background is known to slowly drift with time, the roll minimum backgrounds can only be used for dates close in time to the calibration roll maneuvers. Therefore, a method is needed to extrapolate the roll minimum backgrounds to other dates. Also, it was found that, while the roll minimum backgrounds are more successful in the equatorial regions, the monthly minimum backgrounds are more successful in the polar coronal hole regions. Thus, a method was developed to combine the information from the calibration rolls with the existing monthly minimum backgrounds.

For each monthly minimum background image, a calibration roll background image is calculated by interpolating between the two closest calibration roll maneuvers. The calibration roll data are then intensity scaled to the monthly minimum image by calculating the

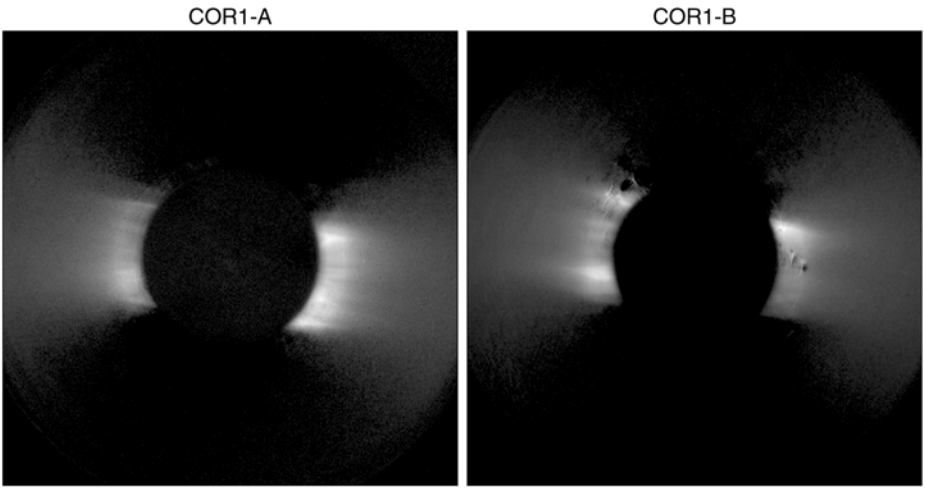

Figure 6 Difference images formed by subtracting from a COR1 monthly minimum background, the same background combined with calibration roll data, for 3 June 2008.

average ratio between the two over the unvignetted part of each image, *i.e.* where the flat field value is close to one. A new combined background is then calculated by taking the pixel-by-pixel minimum between the two images. The additional K coronal light that is rejected in this combined background is demonstrated in Figure 6. The resulting background, shown in Figure 7, shows no evidence of any residual K corona in *pB* (compare Figures 1 and 7). The improvement in the background subtraction can also be seen when applied to the data, as shown in Figure 8. These combined backgrounds are generated for the same dates as the regular monthly minimum backgrounds, *i.e.* every 10 days. In `SECCHI_PREP`, the combined backgrounds are invoked with the keyword `/CALROLL`.

No calibration rolls were performed between early 2007 and early 2008. Because of this fact, use of the /CALROLL keyword is not recommended for dates in 2007, unless relatively close to an appropriate calibration roll. The schedule of calibration rolls is discussed in more detail in the following section.

5. Relationship with Spacecraft Events

The importance of the calibration rolls was not initially recognized. Early in the mission, the pointings of both spacecraft were adjusted several times to optimize the stray light in the COR2 telescopes. Calibration rolls were made soon after the spacecraft pointings were finalized, but no additional calibration rolls were performed until January 2008, when a program of performing roll maneuvers on a regular basis was instituted. Calibration rolls are now performed approximately four times a year, at spacecraft perihelion, aphelion, and at the midpoints between perihelion and aphelion. Table 1 shows the relationship between calibration rolls and spacecraft events (such as repointings) which affect the COR1 scattered light background. It proved possible to derive roll minimum background images from the combination of a couple of S/WAVES (Bougeret *et al.*, 2008) roll maneuvers on STEREO-B in January 2007, so this also appears as an event in Table 1.

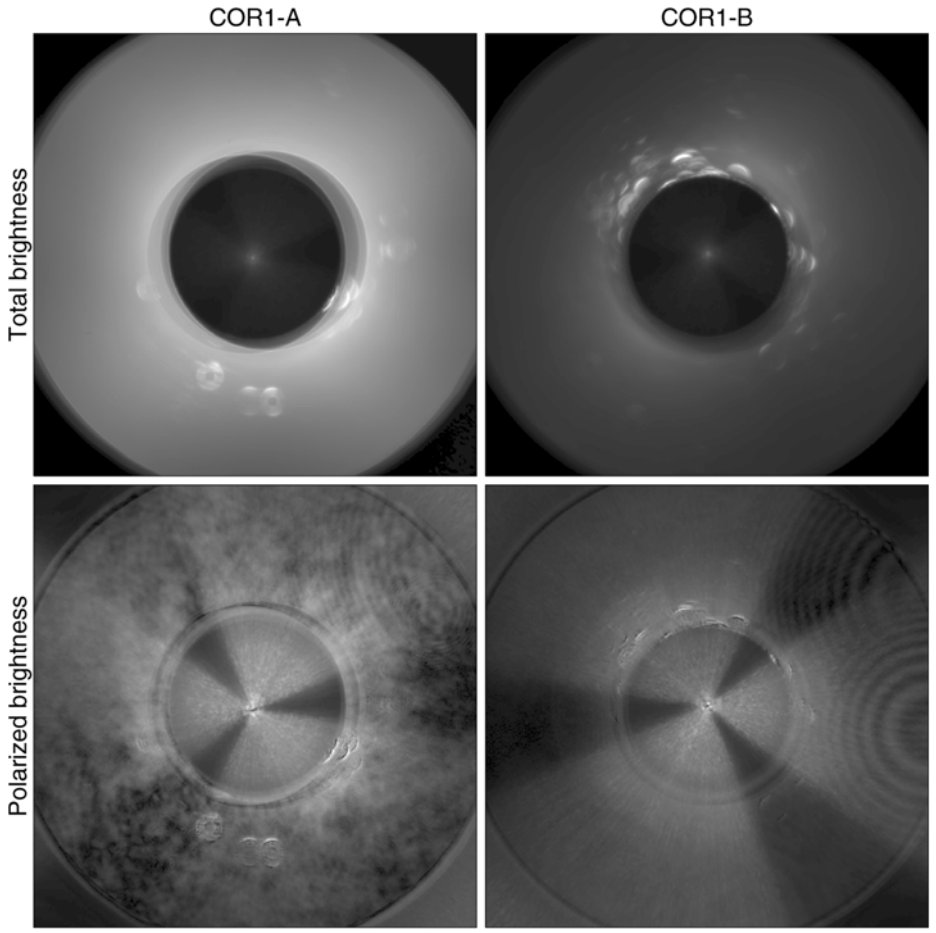

Figure 7 Total and polarized components of the COR1 background images combined from both monthly minimum images and calibration rolls, for 3 June 2008. Compare with Figure 1.

The COR1 scattered light background depends strongly on the spacecraft pointing. A clear demarcation needs to be made between the background data from before the repoint and after the repoint. Because of this, the background subtraction close to a repoint event will be poorer than normal, as it will not be generated from a full 29 days' worth of data.

On 30 January 2009, the COR1-B background increased suddenly, most likely due to the deposition of a ~ 100 μm particle on the objective lens. This is treated by the software as being equivalent to a repoint. Section 6 describes this event in more detail.

On 19 April 2009, the amount of onboard binning applied to the COR1 data was increased to bring down 512×512 images instead of the 1024×1024 format that had been used previously. This was done to handle the declining telemetry rate as the two spacecraft separate from Earth, and to increase the normal cadence from one observation every 10 minutes to one every 5 minutes. This also needed to be partially treated as a repoint by the software. If one attempts to generate monthly minimum images from a mixture of resolutions, or apply lower resolution backgrounds to higher resolution data, then aliasing occurs.

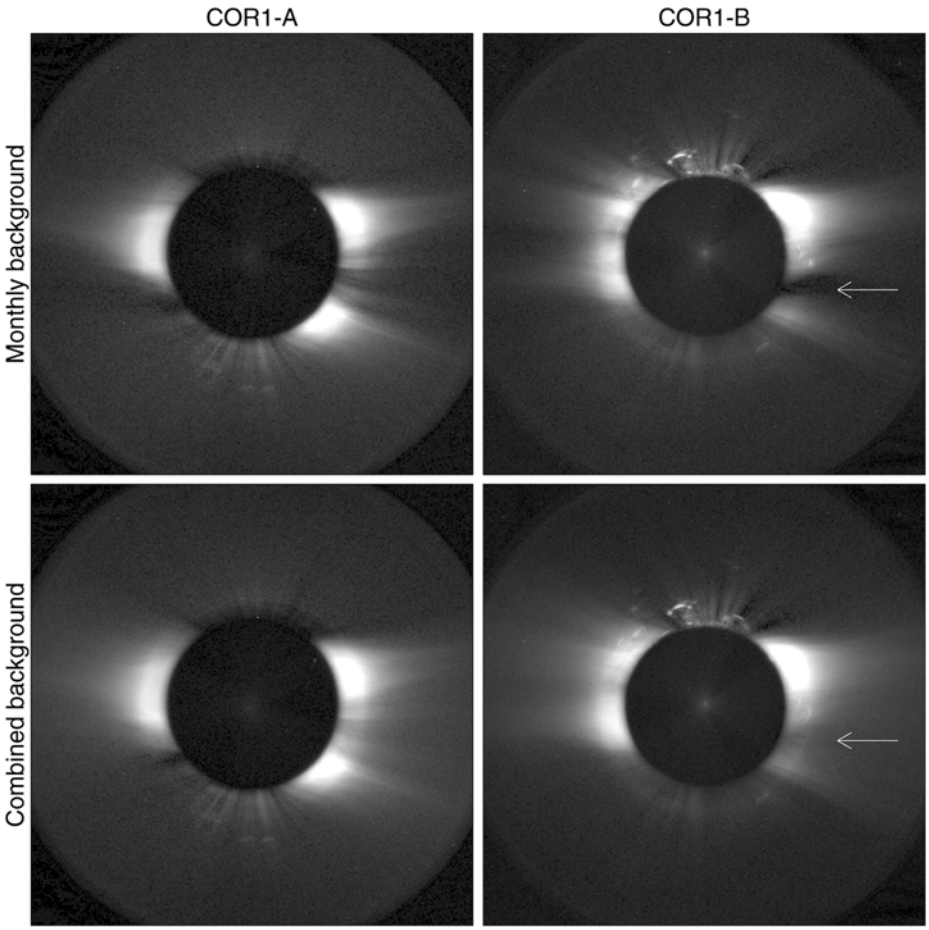

Figure 8 Sample COR1 images processed with both the regular monthly minimum background images (top row) and the combined background images using the calibration roll data (bottom row). The arrow points to a dark lane which is not seen when the combined background is applied to the data.

Therefore, the backgrounds applied to the data must be derived from data taken at the same resolution. The one exception is the calibration roll data; it proved possible to downsize the 1024×1024 roll minimum data to the lower 512×512 resolution to generate the combined backgrounds discussed in Section 4.

6. Discontinuous Change in COR1-B Scattered Light

On 30 January 2009, the COR1-B scattered light background suddenly changed between successive images taken at 16:15 and 16:25 UT, as demonstrated in Figure 9. The difference between the two times, shown on the right side of Figure 9, is consistent with a single scattering source near the edge of the objective lens. The most reasonable explanations are that either a small piece of dust of about 100 µm in size adhered to the front objective, or a micrometeorite caused a small fracture in the objective. Some slight downward evolution was seen in the brightness of this new scattering feature over the first few hours after it appeared.

Table 1 Events which affect the COR1 background subtraction, up through April 2009. A horizontal line marks the start of regularly scheduled calibration roll maneuvers four times a year.

Date	STEREO-A events	Date	STEREO-B events
2006-12-21	Repoint	2007-01-30	S/WAVES rolls (on 29th & 31st)
2007-02-03	Repoint	2007-02-03	Repoint
2007-02-20	Calibration roll	2007-02-06	Calibration roll
		2007-02-21	Repoint
		2007-04-17	Calibration roll
2008-01-03	Calibration roll	2008-02-19	Calibration roll
2008-04-01	Calibration roll		
2008-06-26	Calibration roll	2008-06-25	Calibration roll
2008-09-30	Calibration roll	2008-08-26	Calibration roll
2008-12-02	Calibration roll	2008-12-16	Calibration roll
		2009-01-30	Change in background
		2009-02-17	Calibration roll
2009-03-10	Calibration roll	2009-04-07	Calibration roll
2009-04-19	Change to 512 × 512	2009-04-19	Change to 512 × 512

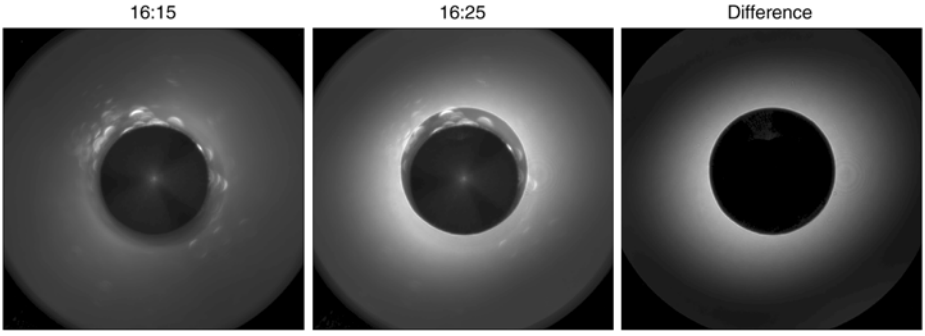

Figure 9 Images showing sudden change in COR1-B background between 16:15 and 16:25 UT on 30 January 2009. On the right is the difference between the two times.

This is felt to be more consistent with the dust hypothesis than the fracture hypothesis. Originally, the COR1-B objective was significantly cleaner than the COR1-A objective; with the new scattering center they now have comparable scattering levels, as demonstrated in Figure 10.

Although the change in total brightness shown in Figure 9 is relatively simple, the change in polarized brightness is quite a bit more complicated. The polarization properties of the scattered light changes not only in magnitude, but in direction as well. This makes it even more important that all three components of the polarized background be subtracted off from an image to derive B and pB for the K corona.

7. Time Dependence

From the monthly minimum background images discussed in Section 2.2, it is possible to examine the variation of the COR1 background over the course of the mission. Figure 11

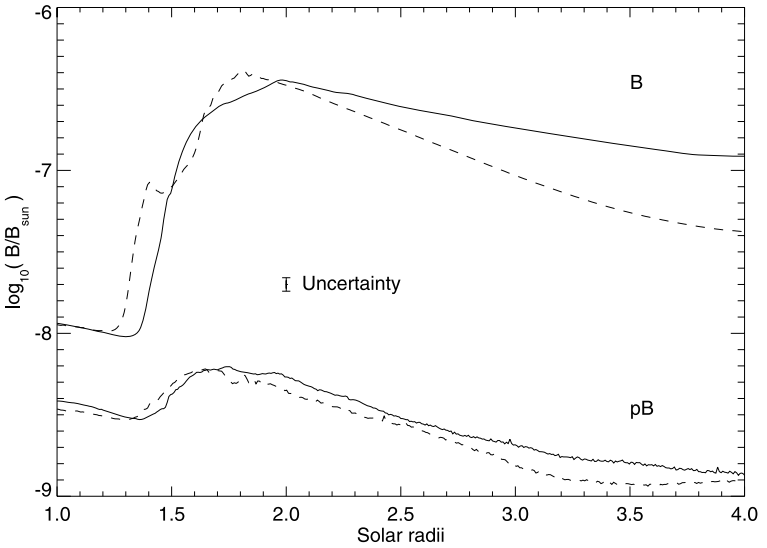

Figure 10 Average radial scattered light profile for COR1-A (solid) and COR1-B (dashed) after 30 January 2009. Compare with Figure 2. The error bar represents 10% radiometric uncertainty.

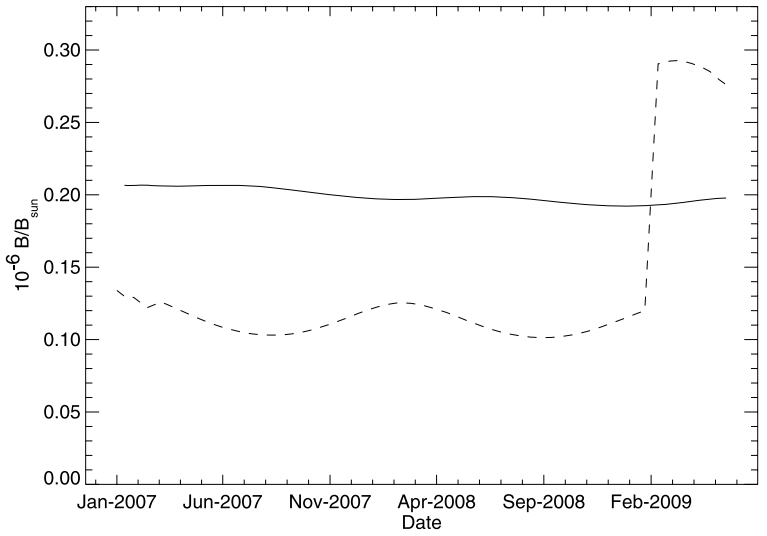

Figure 11 Variation of the average background with time for COR1-A (solid) and COR1-B (dashed).

shows the average background level over the unocculted portion of the image. Several features are evident from this plot. First of all, the sudden change in the COR1-B background on 30 January 2009 is clearly evident. The next most visible feature is a sinusoidal variation, which is caused by the varying solar distance over the course of a spacecraft year. STEREO-B's orbit is more eccentric than that of STEREO-A, so the annual variation is more evident

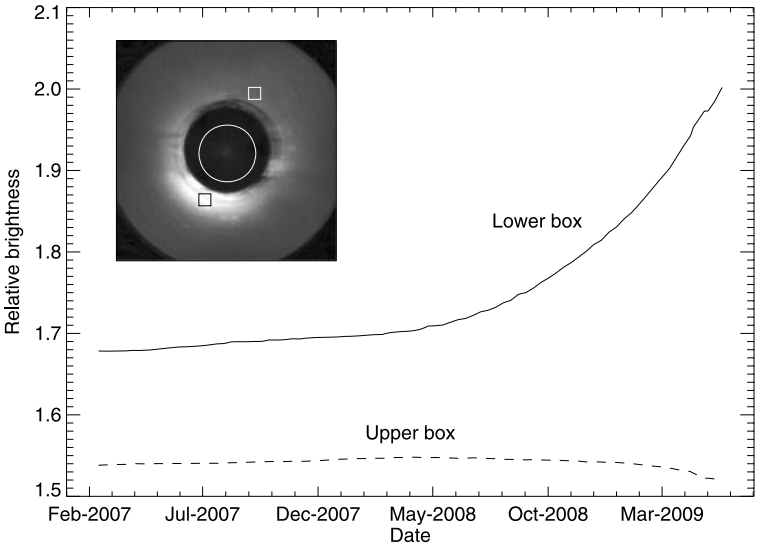

Figure 12 Variation of the COR1-A background for two regions, relative to the overall background variation from Figure 11. The inset image is the difference between two background images separated by 20 days in March 2009. The circle shows the position of the Sun behind the occulter.

for COR1-B. A small jag in the COR1-B plot near February 2007 is due to a change in the spacecraft pointing around that time.

Finally, there is a small but discernible downward drift in background intensity for both spacecraft, of about 3 – 4% per year. Monitoring of star brightnesses shows that this drift is an actual decrease in the scattered light levels, and not a change in the instrument sensitivity. We believe that the objective lenses are slowly cleaning themselves of contaminants, possibly through a process known as plasma cleaning (Flanagan and Goree, 2006). Indeed, there was a significant drop of about 15% in the scattered light levels for both COR1 telescopes within a few days after the instrument doors were first opened in December 2006.

The most recent COR1-A images show significant evolution in the region just to the southeast of the occulter, as demonstrated in Figure 12. Because this region is changing brightness significantly with time, it is proving difficult to remove in the standard background analysis. However, this extra scattered light is completely unpolarized, and does not show up in *pB* images.

It is not yet clear what is causing this new feature. Preferential scattering directions from the objective were seen during instrument development, but these features always exhibited 180° symmetry, and would extend outward to the edge of the field of view. We also considered the possibility of a change in the pointing of COR1 relative to the other telescopes, but this would appear as a brightening on one side of the occulter, and a corresponding dimming on the other side. The two regions tracked in Figure 12 demonstrate that this is not the case. One clue to the nature of this artifact is that it appears to be restricted to a circular region a little larger than two solar radii in size, which is offset from sun center by not quite 4 arcminutes. We are considering the possibility that this is some kind of ghost image appearing in the optics, although why it would be time dependent is unclear.

8. Comparison with MLSO

To test the effectiveness of the COR1 background removal, we compared the COR1 polarized brightness images with simultaneous measurements from the Mauna Loa Solar Observatory (MLSO) Mk4 coronagraph (Elmore *et al.*, 2003). A more comprehensive comparison of COR1 to other coronagraphs is given in Frazin *et al.* (2010). Data from 2 April 2007 was chosen as a period when good backgrounds should be available, and when the separation angles were relatively small, about 3° between STEREO-A and B. The relevant calibration roll on STEREO-A was 41 days earlier, which is close enough in time to be useful. The calibration roll on STEREO-B was just 15 days after the selected date. The COR1 data was processed using the `/CALROLL` and `/INTERPOLATE` keywords to use the combined backgrounds discussed in Section 4, and to interpolate between the 10-day background files. The Mauna Loa image, shown in Figure 13 is an average of 16 images between 17:47 and 18:57 UT. The COR1 images were both taken at 18:10 UT. The COR1 bandpass is 22.5 nm wide centered at 659 nm, while the Mk4 bandpass is somewhat redder, with a principal wavelength of 775 nm. This is not expected to significantly affect the comparison.

The intercomparison of the COR1 and Mk4 data are sensitive to the pointing and plate-scale calibrations of the two instruments. The pointing and plate-scale properties of COR1 are known to 1 – 2 arcsecond accuracy over the whole image through star observations. However, there is some doubt about the accuracy of the Mk4 plate scale. The value in the file header is 6.00 arcseconds per pixel, but recent analysis of lunar eclipse observations imply that the true plate scale should be closer to 5.81 ± 0.07 arcseconds per pixel. We will discuss the implications of both plate scales, although for simplicity only the data using the value in the file header will be shown in the plots. The pointing accuracy of Mk4 data is on the order of ± 20 arcseconds (Elmore *et al.*, 2003), which should not significantly affect the comparison.

Figure 14 shows *pB* at three selected solar radii as measured by all three coronagraphs. The Mk4 data have been shifted by 2.5° to correct for an apparent offset in roll. The source for this roll offset has since been identified by the MLSO team, and they are in the process of correcting the Mk4 data to remove this error. It is clear that the three coronagraphs match each other very well in shape, but the Mk4 values are higher than those of either COR1 telescope almost everywhere when the standard Mk4 plate scale of 6.00 arcsec pixel^{-1} is used. If the plate scale of 5.81 arcsec pixel^{-1} were used instead, then the Mk4 and COR1 values would match better in the streamers, but the Mk4 values would still be higher than

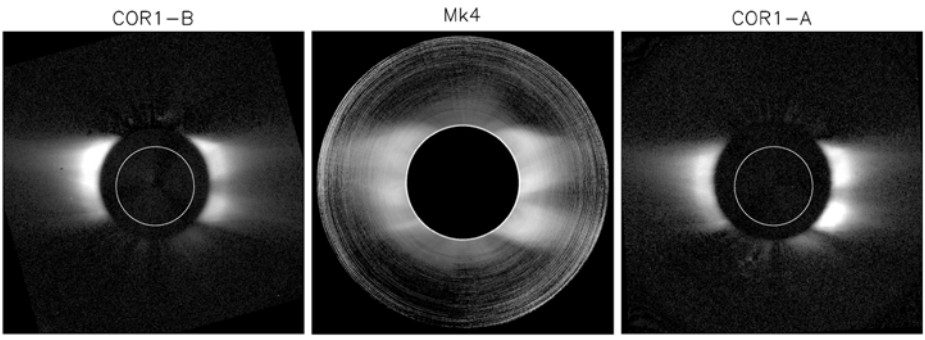

Figure 13 Simultaneous images from the MLSO Mk4 and the two COR1 coronagraphs. The images are not to scale, and have been processed to bring out the fainter features.

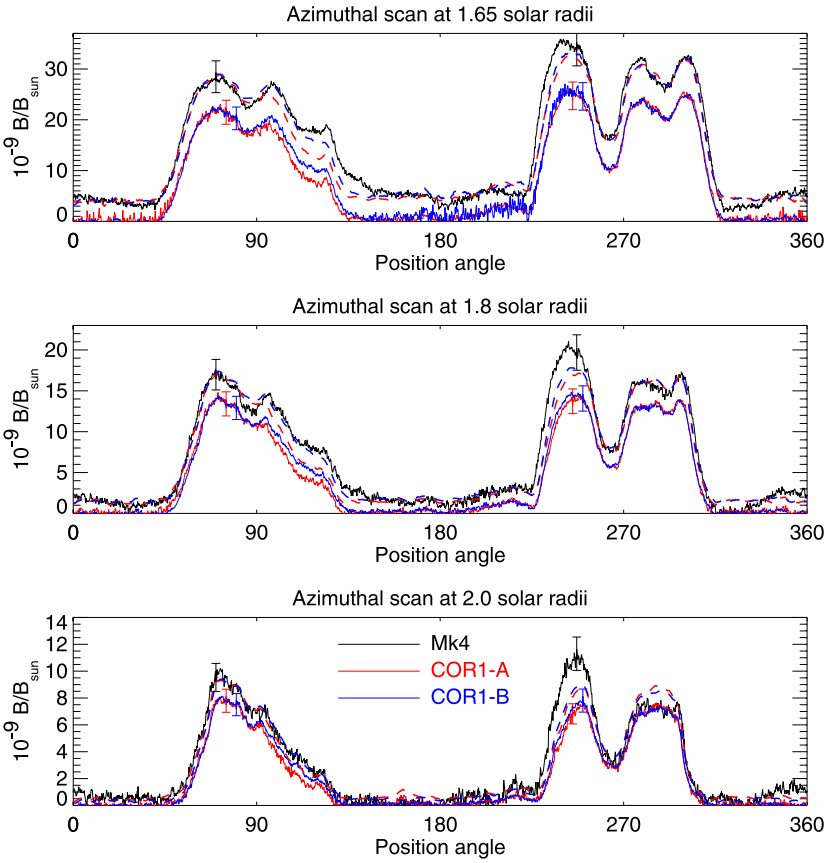

Figure 14 Comparison of polarized brightness measurements made by the MLSO Mk4 (black) with those from COR1-A (red) and COR1-B (blue), as a function of position angle at various radial distances. Each scan is an average over 0.2 solar radii. The dashed lines represent fits to the COR1 data to best match the Mk4 values over most of the range. The fits have been smoothed for ease of reading. Sample error bars represent the radiometric uncertainty for each telescope.

COR1 in the polar regions. The two COR1 measurements track each other very well. One question that arises is what part of the difference is due to the COR1 background subtraction procedure, and what part is due to a difference in the radiometric calibration between the coronagraphs. In Paper I, it was reported that the Mk4 values were higher than those of COR1, but that it was difficult to be precise because of the faintness of the CME being used, and interference from residual sky polarization.

To explore the relative importance of the radiometric calibration and background subtraction, we searched for linear fits of the form $a \times \mathrm{COR1} + b$ which matched the Mk4 data in Figure 14 over most of the range. By first treating each trace separately, we found slopes a between 1.066 and 1.151, with a mean of 1.124 ± 0.031 when using the standard plate scale. If we assume the plate scale is instead 5.81 arcsec pixel^{-1}, then we derive a slope of 0.921 ± 0.042. We then held $a = 1.124$ (or 0.921) constant (*i.e.* assumed that the radiometric calibration of the Mk4 is 12.4% higher (or 7.9% lower) than COR1). From this we determined the average offsets b, listed in Table 2, which are interpreted as background subtraction errors. The resulting fits are shown as the dashed lines in Figure 14. However, even

Table 2 Average intensity differences between the Mk4 AND COR1 after applying a radiometric adjustment of 12.4% or −9.2% respectively, in units of $B/B_{\odot}$ for two different values of the Mk4 plate scale.

Solar radii	6.00 arcsec pixel^{-1}		5.81 arcsec pixel^{-1}	
	COR1-A	COR1-B	COR1-A	COR1-B
1.65	4.066×10^{-9}	4.154×10^{-9}	2.440×10^{-9}	2.615×10^{-9}
1.8	1.304×10^{-9}	1.522×10^{-9}	1.069×10^{-9}	9.38×10^{-10}
2.0	5.33×10^{-10}	4.03×10^{-10}	3.61×10^{-10}	2.75×10^{-10}

with the adjustments, there are areas of disagreement, particularly at 245° where the Mk4 values are always higher. The same is true when the alternate Mk4 plate scale of 5.81 arcsec pixel^{-1} is used – the qualitative relationship between the Mk4 curves and the dashed line fits is insensitive to which plate-scale value is used.

Within the polar coronal holes, the COR1 values go to essentially zero. This is to be expected from the way that the backgrounds are derived. (Features above the base value, such as polar plumes, are still detectable.) The data have also been processed to remove apparent polarization induced by noise at low signal levels by using the SolarSoft routine `COR1_FITPOL`. This routine fixes the direction of polarization to be tangential to the solar limb, and treats the determination of *pB* as a least-squares problem. When the signal strength is high, there is no significant difference between the calculation performed by `COR1_FITPOL` and the standard *pB* calculation (Billings, 1966). However, when the signal is noise dominated, `COR1_FITPOL` will tend to suppress any spurious *pB* signals. This is particularly true when pixels are averaged together. This is because `COR1_FITPOL` can return both positive and negative *pB* values, where the sign represents tangential and radial polarization respectively. When pixels are averaged together in noise-dominated regions, the positive and negative values will tend to cancel out, thus beating down the noise.

The behavior with radius is demonstrated in Figure 15, where the data are averaged over azimuthal ranges of 15° centered on the bright coronal streamers. At 90° and 245°, the COR1 and Mk4 data show essentially the same behavior with radius, but with the Mk4 values being higher. At 280°, the Mk4 values fall more swiftly than the COR1 values, and also more swiftly than the other two streamers. The Mk4 and COR1 match better if the alternate Mk4 plate scale of 5.81 arcsec pixel^{-1} is used, but the overall behavior is the same.

9. Conclusions

We have demonstrated a procedure for removing the instrumental and F coronal background from COR1 observations. The standard background calibration is based on the analysis of the data over a complete solar rotation, as has been done before for the LASCO/C2 and C3 coronagraphs. Significant improvements can be made by folding in information from periodic calibration roll maneuvers. Additional improvements are made by using the SolarSoft routine `COR1_FITPOL` which suppresses noise-generated *pB* signals.

Comparison with the MLSO Mk4 coronagraph shows that the same coronal features are observed by all three telescopes. The best agreement between the two COR1 telescopes and the Mk4 was found by assuming that the radiometric calibration of the Mk4 was 10 – 15% higher than COR1 (or 5 – 10% lower if the alternate Mk4 plate scale of 5.81 was used), and that an additional K coronal signal needed to be added as a function of radial distance. It should be noted that Paper I, which used a completely different technique to compare the

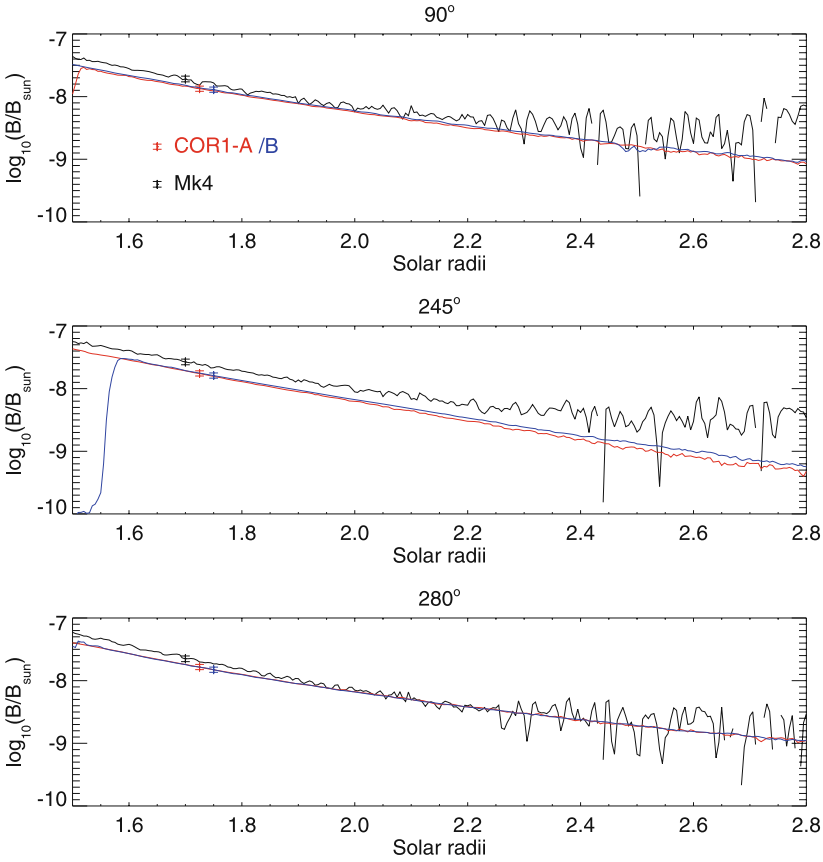

Figure 15 Comparison of polarized brightness measurements as a function of radius at several position angles representing coronal streamers. Colors are the same as in Figure 14. Sample error bars represent the radiometric uncertainty for each telescope. At the larger radial distances, the Mk4 uncertainties increase due to sky scattering effects.

radiometric response, also found that the Mk4 response was higher than that of COR1, while the response of the LASCO/C2 telescope (Brueckner *et al.*, 1995) was about 20% lower. The quoted uncertainties in the calibrations are 11% for the Mk4 (Elmore *et al.*, 2003), and 10% for COR1 (Thompson and Reginald, 2008); therefore the COR1 and Mk4 measurements are consistent within these uncertainties, regardless of which Mk4 plate scale is used. Frazin *et al.* (2002) remarks that the LASCO/C2 vignetting correction appeared to be $\sim$30% too low at the heights at which the Paper I comparisons were made, which is consistent with the Paper I results. The subsequent changes in the LASCO/C2 vignetting correction have been examined, and are insufficient to explain the Frazin *et al.* (2002) findings.

The need to include an additional K coronal signal as a function of radial distance is to be expected from the way the COR1 backgrounds are derived. The incorporation of the calibration roll maneuvers into the background calculations means essentially that the polar coronal holes are used as a reference to which the rest of the corona is compared. Therefore, one would expect that the measured signal would be lower than the actual K corona at all azimuths by an amount equal to the base signal in the polar coronal holes. Comparison with

the Mk4 showed this to be qualitatively true, with localized regions being either somewhat higher or lower in the Mk4 compared to either COR1 telescope. Localized errors in the COR1 background subtraction affect this result, as does the uncertainty in the Mk4/COR1 intercalibration.

Although the COR1 background subtraction method causes the base brightness in polar coronal holes to be close to zero, individual features can still be detected within the polar regions. Polar plumes are quite visible in COR1 images, and can be easily tracked with the solar rotation. Polar jets are easily detected, and are often seen in COR1 movies.

The scattered light behavior of both COR1 telescopes has proven to be quite steady in time, with the notable exception of a single contamination event for COR1-B on 30 January 2009. Also, a localized region in the COR1-A data shows a slow but steady increase in time; the reason for this is still under investigation. Otherwise, the general levels of scattered light are actually decreasing slightly with time, rather than increasing. Barring too many additional events of the sort that occurred on 30 January 2009, there is every reason to believe that both COR1 telescopes will maintain usable levels of scattered light for the remainder of the STEREO mission.

COR1 background files are distributed as part of the SolarSoft Database package available at www.lmsal.com/solarsoft/sswdb_description.html. The background files are organized into four components for each spacecraft: `daily_med` for the daily "median" backgrounds, `monthly_min` for the monthly minimum backgrounds, `roll_min` for the calibration roll backgrounds, and `monthly_roll` for the combined backgrounds. For most users, only the `monthly_min` and `monthly_roll` directories are needed.

Acknowledgements The authors would like to thank Karl Battams for discussions on the LASCO background subtraction technique. They would also like to thank the referee for many helpful suggestions. The STEREO/SECCHI data used here are produced by an international consortium of the Naval Research Laboratory (USA), Lockheed Martin Solar and Astrophysics Lab (USA), NASA Goddard Space Flight Center (USA), Rutherford Appleton Laboratory (UK), University of Birmingham (UK), Max-Planck-Institut für Sonnensystemforschung (Germany), Centre Spatiale de Liège (Belgium), Institut d'Optique Théorique et Appliquée (France), Institut d'Astrophysique Spatiale (France). This work was supported by NASA grant NNG06EB68C.

References

Billings D.E.: 1966, *A Guide to the Solar Corona*. Academic Press, New York.

Bougeret, J.L., Goetz, K., Kaiser, M.L., Bale, S.D., Kellogg, P.J., Maksimovic, M., Monge, N., Monson, S.J., Astier, P.L., Davy, S., Dekkali, M., Hinze, J.J., Manning, R.E., Aguilar-Rodriguez, E., Bonnin, X., Briand, C., Cairns, I.H., Cattell, C.A., Cecconi, B., Eastwood, J., Ergun, R.E., Fainberg, J., Hoang, S., Huttunen, K.E.J., Krucker, S., Lecacheux, A., MacDowall, R.J., Macher, W., Mangeney, A., Meetre, C.A., Moussas, X., Nguyen, Q.N., Oswald, T.H., Pulupa, M., Reiner, M.J., Robinson, P.A., Rucker, H., Salem, C., Santolik, O., Silvis, J.M., Ullrich, R., Zarka, P., Zouganelis, I.: 2008, S/WAVES: The radio and plasma wave investigation on the STEREO mission. *Space Sci. Rev.* **136**, 487 – 528. doi:10.1007/s11214-007-9298-8.

Brueckner, G.E., Howard, R.A., Koomen, M.J., Korendyke, C.M., Michels, D.J., Moses, J.D., Socker, D.G., Dere, K.P., Lamy, P.L., Llebaria, A., Bout, M.V., Schwenn, R., Simnett, G.M., Bedford, D.K., Eyles, C.J.: 1995, The Large Angle Spectroscopic Coronagraph (LASCO). *Solar Phys.* **162**, 357 – 402. doi:10.1007/BF00733434.

Elmore D.F., Burkepile J.T., Darnell J.A., Lecinski A.R., Stanger A.L.: 2003, Calibration of a ground-based solar coronal polarimeter. In: Fineschi, S. (ed.) *Polarimetry in Astronomy, Proc. SPIE* **4843**, 66 – 75.

Flanagan, T.M., Goree, J.: 2006, Dust release from surfaces exposed to plasma. *Phys. Plasmas* **13**(12), 123504. doi:10.1063/1.2401155.

Frazin, R.A., Romoli, M., Kohl, J.L., Gardner, L.D., Wang, D., Howard, R.A., Kucera, T.A.: 2002, White light intercalibrations of UVCS, LASCO-C2 and Spartan 201/WLC. In: Pauluhn, A., Huber, M.C.E., von Steiger, R. (eds.) *The Radiometric Calibration of SOHO (ESA SR-002)* **2**, 249 – 263.

Frazin R.A., Vásquez A.M., Thompson W.T., Lamy P., Llebaria A., Burkepile J., Elmore D., Hewett R., Kamalabadi F.: 2010, Intercomparison of the STEREO, SOHO and MLSO coronagraphs and the POISE eclipse instrument. *Solar Phys.*, to be submitted.

Freeland, S.L., Handy, B.N.: 1998, Data analysis with the SolarSoft system. *Solar Phys.* **182**, 497 – 500.

Howard, R.A., Moses, J., Vourlidas, A., Newmark, J., Socker, D., Plunkett, S., Korendyke, C., Cook, J.W., Hurley, A., Davila, J.M., Thompson, W.T., Cyr, O.S., Mentzell, E., Mehalick, K., Lemen, J., Wuelser, J., Duncan, D., Tarbell, T., Wolfson, C., Moore, A., Harrison, R.A., Waltham, N.R., Lang, J., Davis, C., Eyles, C., Mapson-Menard, H., Simnett, G., Halain, J., Defise, J., Mazy, E., Rochus, P., Mercier, R., Ravet, M.F., Delmotte, F., Auchère, F., Delaboudinière, J.-P., Bothmer, V., Deutsch, W., Wang, D., Rich, N., Cooper, S., Stephens, V., Maahs, G., Baugh, R., Mcmullin, D.: 2008, Sun Earth Connection Coronal and Heliospheric Investigation (SECCHI). *Space Sci. Rev.* **136**, 67 – 115.

Lyot, B.: 1939, The study of the solar corona and prominences without eclipses (George Darwin Lecture, 1939). *Mon. Not. Roy. Astron. Soc.* **99**, 580 – 594.

Morrill, J.S., Korendyke, C.M., Brueckner, G.E., Giovane, F., Howard, R.A., Koomen, M., Moses, D., Plunkett, S.P., Vourlidas, A., Esfandiari, E., Rich, N., Wang, D., Thernisien, A.F., Lamy, P., Llebaria, A., Biesecker, D., Michels, D., Gong, Q., Andrews, M.: 2006, Calibration of the SOHO/LASCO C3 white light coronagraph. *Solar Phys.* **233**, 331 – 372.

Thompson W.T., Davila J.M., Fisher R.R., Orwig L.E., Mentzell J.E., Hetherington S.E., Derro R.J., Federline R.E., Clark D.C., Chen P.T.C., Tveekrem J.L., Martino A.J., Novello J., Wesenberg R.P., StCyr O.C., Reginald N.L., Howard R.A., Mehalick K.I., Hersh M.J., Newman M.D., Thomas D.L., Card G.L., Elmore D.F.: 2003, COR1 inner coronagraph for STEREO-SECCHI. In: Keil, S.L., Avakyan, S.V. (eds.) *Innovative Telescopes and Instrumentation for Solar Astrophysics, Proc. SPIE* **4853**, 1 – 11.

Thompson, W.T., Reginald, N.L.: 2008, The radiometric and pointing calibration of SECCHI COR1 on STEREO. *Solar Phys.* **250**, 443 – 454.